2003-01-0422

Cold Start Fuel Economy and Power Limitations for a PEM Fuel Cell Vehicle

Stephen D. Gurski and Douglas J. Nelson
Mechanical Engineering, Virginia Tech
Blacksburg VA, 24061

ABSTRACT

Fuel cells are being considered for transportation primarily because they have the ability to increase vehicle energy efficiency and significantly reduce or eliminate tailpipe emissions. A proton exchange membrane fuel cell is an electrochemical device for which the operational characteristics depend heavily upon temperature. Thus, it is important to know how the thermal design of the system affects the performance and efficiency of a fuel cell vehicle. More specifically, this work addresses issues of the initial thermal transient known to the automotive community as "cold start" effects for a direct hydrogen fuel cell system. Cold start effects play a significant role in power limitations in a fuel cell vehicle, and may require hybridization (batteries) to supplement available power. The results include a comparison of cold-start and hot-start fuel cell power, efficiency and fuel economy for a hybrid fuel cell vehicle.

Fuel cell system design can significantly affect the cold start performance of a fuel cell system. Through modeling, it is possible to quantify the impact of thermal mass on warm up time to operating temperature of a fuel cell system. As expected, performance reduction is seen during cold start that affects both available power and fuel use. The overall cold start energy use penalty is relatively small (~ 5% difference) for the combination of component sizes and control strategy presented here.

INTRODUCTION

Fuel Cell System Model

Understanding the complex interaction between the thermal fluid systems of a fuel cell is needed to quantify the impact that cold start has on vehicle efficiency and performance. A vehicle fuel cell system developed at Virginia Tech is used as a practical example to follow for the system model. The Virginia Tech 50 kW fuel cell system uses a design approach where practicality, simplicity and safety were key requirements. A diagram of the system, shown below in Figure 1, identifies the major system components that are in the physical fuel cell system, and are accounted for in the fuel cell system model.

A fuel cell system can be broken down into three major sub-systems; air supply, coolant loop, and fuel supply. Energy and mass balances for each component are used to model the system. The details and equations used are available in Gurski (2002).

MODEL CAPABILITIES AND OPERATIONAL STRATEGY

To make a fuel cell system useful in a vehicle system, some amount of control over the system is necessary to implement requests from the operating strategy. With laboratory development, the fuel cell system can be characterized and a controller used to change inputs to the system to achieve the desired power generation. However, for this model, a single input iterative approach was chosen for simplicity. In the actual vehicle development, the fuel cell control strategy was based upon a current request to the fuel cell stack. This allows the air compressor speed and humidification for the fuel and air to be set to the appropriate levels.

Safe and proper operation of the fuel cell has constraints such as maximum power and minimum cell voltage; these parameters are usually set by the fuel cell manufacturer and are included in the model. In an effort to increase system efficiency, previous work done by Kulp and Nelson (2001) suggests that a minimum power request be placed upon the system. As part of the implementation into a vehicle simulation tool called ADVISOR, the model needs to handle a net power request. To account for the safe operation requirements and minimum system power, the model uses a goal seeking function to determine a system operating point, given a net power request. The model takes into account the following system electrical parasitics to determine a net power operating point: air compressor, radiator fan, condenser fan and coolant pump.

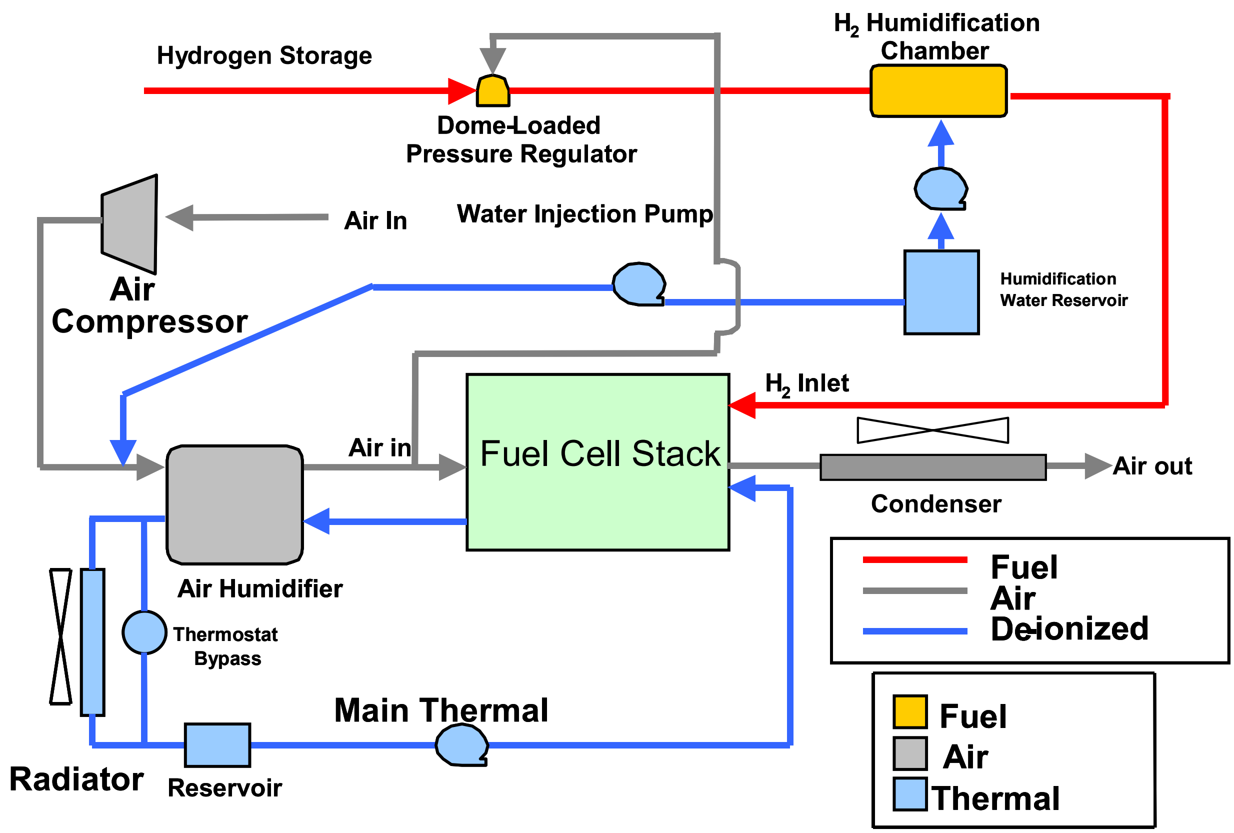

Figure 1. Fuel Cell System Components

The model does the following at each time step:

1. Net power request from vehicle control strategy
2. Guess current density that generates a gross power to meet net power
3. Determine net power operating point
4. Enforce one of the three following limits, through iteration
   A. Generate the net power request, if possible
   B. Impose either a minimum cell voltage or a maximum current density limit that results in limited power output
   C. Generate no power, per minimum power limits from control strategy

The goal of this work is to understand the transient thermal effects that result from limits placed upon fuel cell stack and vehicle operation. Requirement B above can occur for the following reasons:

1. The net power request is much higher than the fuel cell system peak power capability (due to stack sizing and hybridization design).
2. The fuel cell is cold which reduces the stack output voltage
3. Low oxygen content due to air flow and pressurization from the air compressor control

FUEL SYSTEM

A pressurized hydrogen gas storage and delivery system is utilized on-board the vehicle. Hydrogen is humidified and any unused excess is recirculated back into the stack inlet to be reused. Since the hydrogen and water vapor in hydrogen carry comparatively little energy, they have been neglected in the thermal model. From experience, proper design of a direct hydrogen fuel system achieves flow and pressure response that do not limit the fuel cell system response. A dome loaded pressure regulator in the vehicle fuel cell system matches the pressure of the hydrogen to the pressure of the air system. Modeling the dome loaded regulator required the assumption that the hydrogen flow and pressure could be met at all times, and the system model did not utilize recirculation, but rather “dead headed” the fuel cell stacks (the same net effect of recirculation). Purging of hydrogen from the fuel system is not included in the model for the current results.

AIR SYSTEM

Air System - Air Compressor

The air compressor in the system is based on an Opcon 1050 twin screw compressor with an internal compression ratio of 1.44. Empirical data in a 2D lookup table yields the volumetric efficiency, temperature rise and adiabatic efficiency of the compressor as a function of mass flow and outlet pressure. In the vehicle fuel cell system, the compressor works against a fixed orifice that increases the fuel cell operating pressure with an increase in air mass flow. The model control strategy has the ability to change the cathode operating pressure with respect to fuel cell stack current density and fuel cell temperature.

Air System – Humidifier

A liquid-to-air heat exchanger based on an automotive intercooler is utilized as a humidifier in the pressurized air stream. Water is directly injected into the air inlet in the humidifier, and the heat required for vaporization is obtained from the fuel cell coolant running in adjacent flow channels. A simple energy balance between the coolant and the air with humidity water injection is performed. Each of the temperatures and mass flows are obtained from the current operating conditions.

Air System - Condenser

Water balance (water used to humidify inlet air versus water collected from exhaust air) is an issue in practical use and operation of fuel cells for transportation. A simplified air-air heat exchanger with condensation model has been implemented into the system to evaluate water balance. A curve fit based upon empirical data (Kroger, 1984) relates exterior air mass flow to heat transfer capability. The pressure drop across the air side of the condenser is a function of air mass flow, which allows the calculation of power required for the condenser fan. Fan work associated with the condenser is accounted for in the net power calculation of the system.

THERMAL SYSTEM

Thermal System - Coolant Reservoir

In the vehicle system, the pump draws directly from the coolant reservoir. In the model, the coolant reservoir is responsible for the heat lost to the ambient from all of the plumbing, and the lumped capacitance of all the coolant in the system. A backward looking finite difference method and a simple mixed tank model is used to account for the thermal transient of the coolant in the reservoir.

Thermal System - Radiator

The radiator in the system is modeled using a technique similar to that of the condenser in the air system. An energy balance between the coolant and the heat removal capacity of the air flow across the radiator yields the outlet coolant temperature.

The pressure drop across the air side of the radiator is a function of air mass flow, which allows the calculation of power required for the radiator fan. A simple thermostat is part of the radiator model that will not allow heat to be rejected form the radiator below the desired fuel cell operating temperature.

FUEL CELL STACK

The most complex device in the system model is the fuel cell stack. For air reactant flows that are not saturated at the cathode inlet, the system may generate water in vapor form inside the stack. Since the lower heating value of hydrogen is used in the energy balance, the heat generation term assumes that all water product is in vapor form. The water that is generated after the cathode stream is saturated is condensed in the stack, and gives an addition internal heat load term for the stack.

In the model, three streams flow into and two flow out of the stack; the hydrogen outlet has been “dead headed”. To make the system model simpler, the water vapor in air and hydrogen are separated in to flows into the fuel cell stack. Now there are five flows streams in (air, water vapor in air, hydrogen, water vapor in hydrogen, coolant) and three flows out (air, water vapor in air, coolant). All the water vapor in the hydrogen stream is assumed to diffuse through the membrane and exit via the cathode. Making the assumption that a fuel cell stack is an excellent heat and mass exchanger, all of the outlet flows and the stack thermal mass are at the same temperature.

Again, a backward looking finite difference model using a lumped capacitance is used to evaluate the thermal transients in the stack temperature.

OPERATING CONDITIONS

Operating conditions of the fuel cell stack are very important to the performance and thermal response of the system. Listed below are the pertinent base operating conditions for the fuel cell model.

FUEL CELL STACK	
Anode inlet humidity	80% Rh
Cathode inlet humidity	60% Rh
Min cell voltage	0.6 V/cell
Max coolant inlet temperature	80 deg C
Max coolant temp. rise in stack	10 deg C
System Operating Conditions	
Min system power	5000 W
Max fuel cell power	50 kW Net

CHARACTERIZING THE SYSTEM

Before exercising the model in a dynamic vehicle environment, some tests have been performed that describe the system during steady state and simple transients. The first test performed is a steady state characterization of the system parasitic power used to run the fuel cell stack. In Figure 2 below, the parasitic power of the system is determined over the range of net system power up to 50 kW, operating at the base conditions.

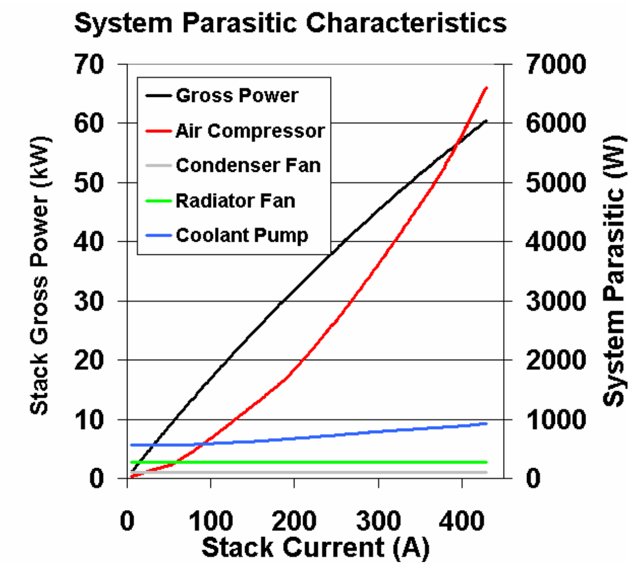

Figure 2. Fuel Cell System Parasitic Power Characteristics

This test was performed at normal operating temperature of 80 deg C. The maximum cathode pressure is 1.8 atm, which corresponds to a stack current of 430 A, or 60 kW of gross power. The minimum stack pressure is 1.05 atm. Note that system component sizing and selection, as well as operating strategy for air flow and pressure as a function of fuel cell current can strongly influence these characteristics.

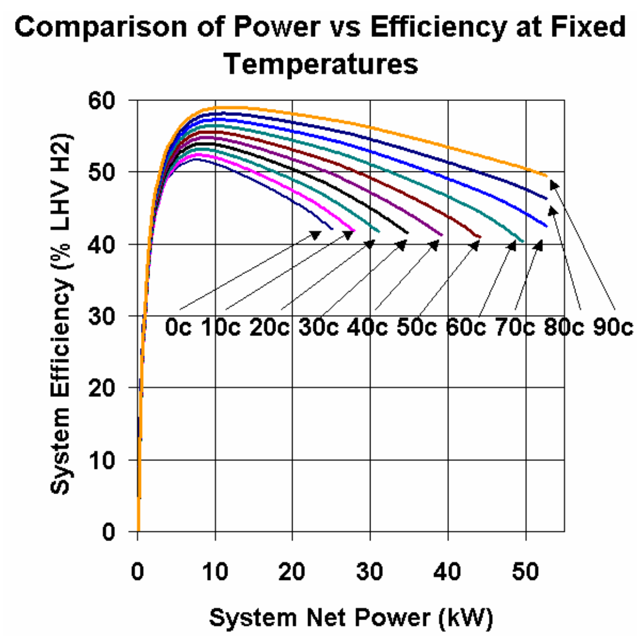

Figure 3. Fuel Cell System Power and Efficiency Variation with Stack Temperature

Characterizing system efficiency and temperature dependence is performed next. Figure 3 shows the system efficiency based on net system power output. Each of the curves represents a different operating temperature and the remaining operating conditions are the same at each power level. For example, at each of the different temperatures operating at 20 kW would have the same cathode pressure, mass flow etc. Each of the efficiency lines end when a minimum cell voltage is encountered. From this figure, the temperature effects are evident in decreasing the available system power and maximum fuel cell system efficiency. In both Figure 2 and Figure 3, the air compressor speed and power were allowed to go to zero; in practice this is difficult to achieve and still have acceptable dynamic response of the system. Figure 3 shows that a minimum power operating strategy can eliminate the low system efficiency region of operation at low loads, which also sets a minimum speed and flow for the air compressor (Kulp et al., 2002).

THERMAL TRANSIENT RESPONSE TO STEP INPUT

Since it is desirable to operate the system at its maximum available efficiency and power, characterizing the thermal transient or cold start performance is necessary. A step power input to the system while requesting the maximum system design power is shown in Figure 4.

When requesting a 50 kW load initially from the fuel cell system, there is a period where net system power is less than requested due to the low stack temperature. For this system, it takes 350 seconds for the fuel cell system to initially warm up to the steady state operating temperature. After 300 seconds, the system has the capability to produce the full rated net power. The temperature limiting effect on power seen in Figure 4 is also seen in the steady state results of Figure 3.

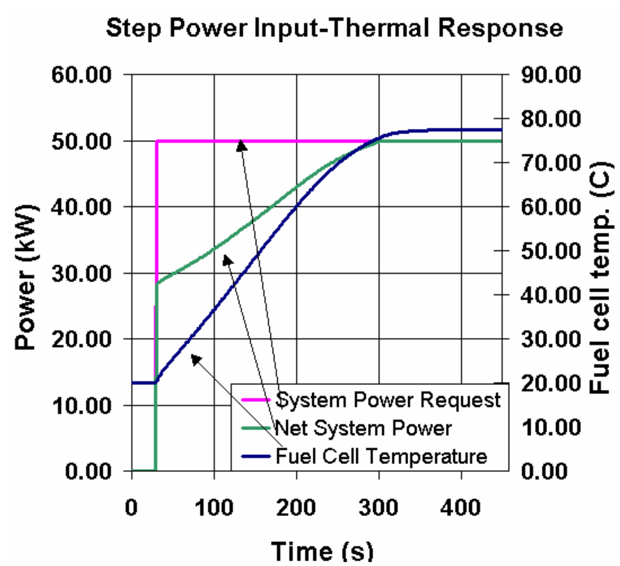

Figure 4. Thermal and Power Response to Step Power Request

VEHICLE MODELING AND ENERGY IMPACT

To understand how the initial cold start transient affects the performance and fuel economy of a vehicle during a drive cycle, the fuel cell system model is incorporated into a vehicle model. The vehicle model is based on a 2002 Ford Explorer that has been converted to a hybrid fuel cell vehicle. Table 1 lists the characteristics of the vehicle used for the drive cycle simulations.

Table 1. Hybrid Fuel Cell Vehicle attributes

Attribute	Value
Mass	2400 kg
Cd	.41
Fa	2.8 m^2
Drivetrain	83 kW GE EV2000
Batteries	16 Ahr 336 V Lead Acid
Fuel Cell	50 kW Net

Table 2 contains performance results of the vehicle model that were obtained using a hot fuel cell system and the performance capability of the 2WD vehicle with a single electric drive axle. Adding a second electric drive axle could improve the performance of the vehicle to levels close to a conventional sport utility vehicle (see Atwood, et al. 2001).

Table 2. Vehicle Performance

Attribute	Model
0-97 kph	18 sec
1/8 mile	15 sec
Gradeability	4.8% @ 55mph

The drive cycle that is used for the hot and cold start comparison is a standard EPA FTP cycle. Using vehicle simulation software called ADVISOR™, the fuel cell vehicle model is used to compare the energy impact for a hot and cold start. Both runs use the same control strategy, and have the same characteristics with the exception of the initial starting temperature. The initial temperature for the cold start is 20 degrees C, and the hot start temperature is 80 degrees C. Also both of the runs are battery state of charge (SOC) corrected for each drive cycle within ½%.

The results show that the cold driving cycle consumed 4.35% more fuel than the hot driving cycle. Taking a closer look at the losses in the system, Figure 5 shows that the majority of the system losses are incurred by the fuel cell system. What is difficult to see in Figure 5 is where the majority of the changes occurred. Table 3 below details how much energy is lost in the system for the duration of the drive cycles. As expected, the majority of the difference comes from the fuel cell operation.

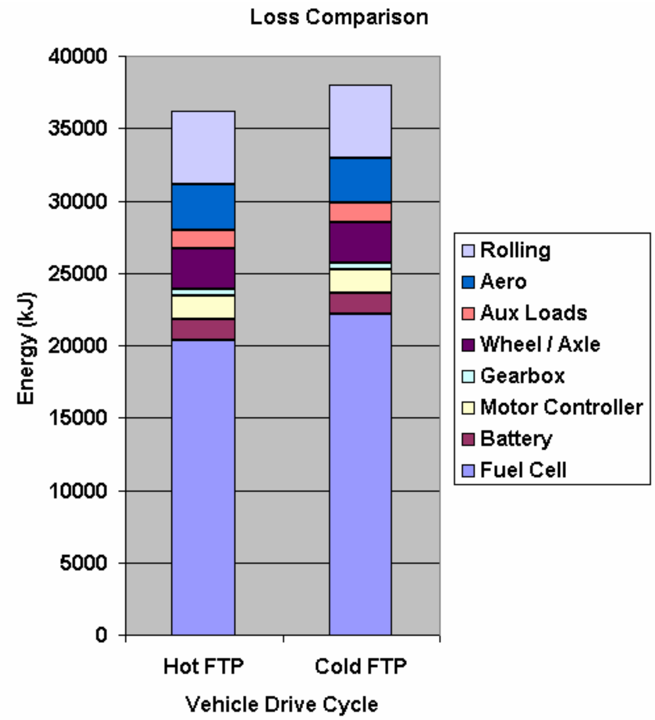

Figure 5. Hot Start and Cold Start Energy Loss Comparison

Table 3. Component Energy Loss Comparison

Component Loss	Hot FTP	Cold FTP	Difference	% of Total Loss
Fuel Cell	20355.00	22145.00	1790.00	94.46
Battery	1455.00	1508.00	53.00	2.8
Motor Controller	1617.00	1598.00	19.00	1.00
Gearbox	432.00	426.00	6.00	0.32
Wheel / Axle	2835.00	2862.00	27.00	1.42
Aux Loads	1314.00	1314.00	0	0
Aero	3130.00	3130.00	0	0
Rolling	5020.00	5020.00	0	0
Total kJ Loss	36158.00	38003.00	1895.00	

Taking a closer look at the fuel cell systems losses, Figure 6 shows that the majority of the losses are accounted for in inefficiencies associated with the fuel cell stack, specifically the energy conversion that generates electrical power.

The fuel cell stack is responsible for the majority of the difference in losses for the hot and cold drive cycles. Figure 7 compares the operating points of the fuel cell stack and the relative efficiencies. Each of the points in Figure 7 represents one second of the drive cycle. The noticeable difference between the two graphs is that the cold FTP has many more operating points occurring at lower efficiencies as the stack warms up.

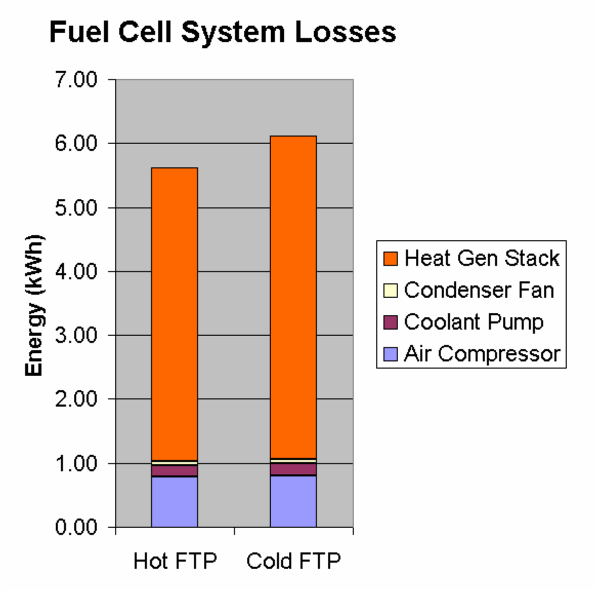

Figure 6. Fuel Cell System Loss Comparison

Thermal effects that change fuel cell stack overpotentials are the dominant cause for the reduction in efficiency and available power. Operating points below the solid line in the figure are not possible because of the minimum cell voltage limitation imposed by the control strategy. This strategy also prevents operation of the stack at lower efficiencies, and so tends to make the cold start energy penalty relatively small.

Another operating limitation of the fuel cell is also seen as a minimum power limit. The fuel cell system incorporates a minimum power level below which the fuel cell does not generate power. As stated before, a minimum system power request can increase the overall system efficiency because the majority of the power generated is allocated to offset parasitics at very low power. This strategy does increase the amount of energy that must be processed through the battery energy storage system, and may increase battery losses as well as sizing requirements (Atwood, et al. 2001).

STANDARD EPA FUEL ECONOMY TEST

To gather an understanding of how this model vehicle compares to that of current production vehicles, the standard EPA fuel economy test has been performed. This is the fuel economy test that yields window sticker (corrected) fuel economy numbers and the published EPA fuel economy results. The test consists of two driving cycles, the FTP-75 and the HWFET.

The EPA test uses a cold start FTP-75 cycle and a hot start HWFET cycle. Fuel economy from the tests are reported here as uncorrected and combined fuel economy. The uncorrected fuel economy figures are simply the raw fuel economy numbers from the FTP-75 and HWFET simulations.

The combined fuel economy number, typically used for annual fuel cost calculations, is a weighted percentage of city and highway fuel economy. For the combined fuel economy, the city accounts for 55% of the total and the remaining 45% comes from the highway results. Table 4 contains the results in miles per gallon of gasoline equivalent energy (MPGGE) from the simulations to yield the fuel economy results for the fuel cell model and the stock vehicle.

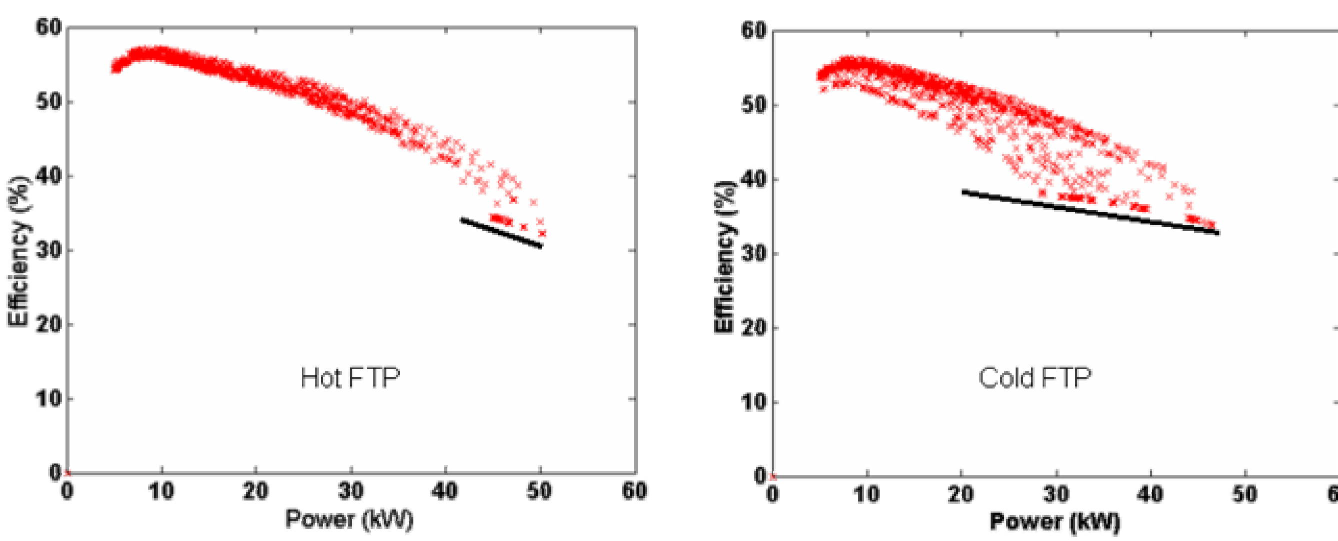

Figure 7. Comparison of Hot and Cold Efficiency Points over a FTP Cycle

Table 4. EPA fuel economy results, MPGGE

Cycle	Raw	Combined
Model: Fuel Cell Vehicle		
FTP-75	34.3	
HWFET	39.2	
Combined		36.3
Production Vehicle: Internal Combustion		
FTP-75	16.9	
HWFET	25.2	
Combined		20.6

The fuel economy results of the fuel cell vehicle are significantly better than that of the production vehicle. Using the combined results, a 77% increase in fuel economy over the production vehicle is accomplished. The performance level of the production vehicle is significantly higher, however, and this accounts for some of the difference in fuel economy.

IMPACT OF POWER LIMITING ON PERFORMANCE

Fuel cell power limiting impacts not only vehicle fuel economy, but also performance metrics such as acceleration and driveablility. To better understand the impact that temperature has on vehicle performance, a full power acceleration 0 to 97 kph (0 to 60 mph) test is performed. The test is performed with the system initially started at 20 deg C (cold) and 80 deg C (hot). At time equal 20 seconds the vehicle performs a maximum power available acceleration. In Figure 8, the results show that the cold start vehicle 0-97 kph time was 8 seconds longer than that of the hot start vehicle. This performance difference could be reduced by increasing the size and power available from the battery, but then this extra battery capacity would go unused most of the time once the vehicle is warmed up.

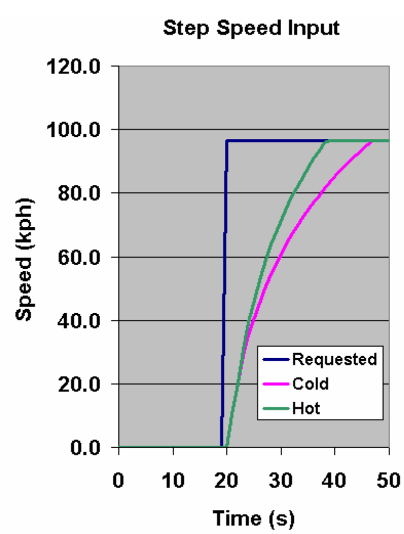

Figure 8. Hot and Cold Acceleration Performance

Figure 9 shows a more dynamic drive cycle example. A US06 drive cycle is used as a comparison because of the more dynamic acceleration, speed and overall aggressiveness relative to that of the standard EPA city and highway drive cycles. A trace miss comparison in Figure 9 shows the degree that the vehicle was unable to maintain the requested speed trace.

The trace miss is the difference between the requested speed during the cycle and the actual speed achieved; taller peaks are larger differences between the requested speed and actual speed. During the 600 second cycle, the first 200 seconds are of most interest because the vehicle had the largest and most frequent trace misses. After 200 seconds both vehicles equally fell short of the request for the drive cycle. Another point to note, during the US06 drive cycle it takes the system approximately 350 seconds to arrive at the desired system operating temperature.

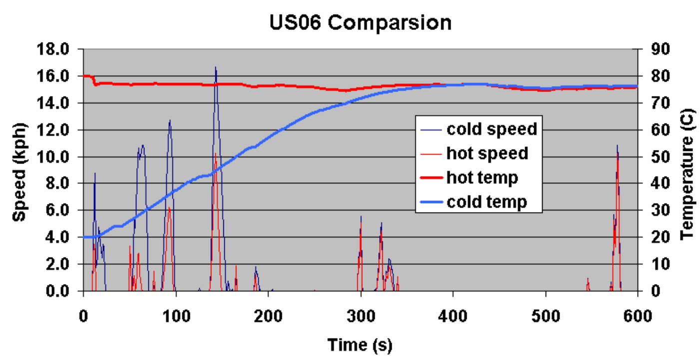

Figure 9. US06 Drive Cycle Hot and Cold

Illustrating the limiting effects of temperature on performance is the intent of evaluating the vehicle on the US06 drive cycle. On an absolute scale, the model vehicle was not able to meet the speed trace criteria of the US06 drive cycle for either hot or cold conditions due to drivetrain component sizing.

The performance limitation of this vehicle during a cold start cycle (inability to meet the speed trace) is attributed to the fuel cell system interaction with the hybridization batteries. To meet the criteria of a SOC corrected drive cycle, the model required a very low initial battery SOC (~45%). The cold start performance of the vehicle further suffers because of power limitations of the batteries at low SOC.

During a hot start US06 drive cycle the vehicle also exhibits performance limitations, although not as extreme as the cold start scenario. During this case, the speed trace miss is not the result of a reduction of performance of the fuel cell system due to temperature. The performance limit is the result of under sizing of the vehicle propulsion system with respect to the vehicle size, weight and performance requirements of the US06 drive cycle.

Several vehicle design modifications can be modeled that would result in a higher performance vehicle capable of meeting the US06 speed trace: increased electric drive power, and increased fuel cell plus battery power. Atwood et al. (2001) present results for a full performance sport utility vehicle for the hot start case.

Energy use summary of EPA and US06 Drive Cycles

Two different drive cycles were used to compare the cold and hot start fuel economy and performance of the modeled fuel cell vehicle. The FTP-75 drive cycle is used to illustrate the differences in a fuel cell vehicle and the US06 is used to compare the performance limitations. Table 5 below is a summary of fuel economy in mpgge.

Table 5. Fuel Economy Comparison of fuel cell vehicle model

	Hot Start	Cold Start
FTP – 75	36.4	34.3
US06	15.5	14.1

CONCLUSIONS

Fuel cell system characteristics and design can significantly affect the cold start performance of a fuel cell system. Through modeling, it is possible to quantify the impact of thermal mass and control strategy on warm up time to operating temperature of a fuel cell system. As expected, a performance reduction is seen during cold start that affects both available power and fuel use. The overall cold start energy use penalty is relatively small for the combination of component sizes and control strategy presented here. Changing the fuel cell system design and operating control strategy could reduce the effects of cold start. One of the challenges in fuel cell vehicle design is the fuel cell stack size necessary to achieve a power level useful in a vehicle. In this model, the majority of the thermal capacitance of the system is tied up in the fuel cell stack and bipolar plates. Industry goals include increasing the power density, which would result in a decreased stack size with subsequent reduction in thermal mass of a fuel cell system.

Future work to reduce cold start effects using this model would be to explore the operating control strategies. Use of additional fuel cell stack power that potentially could be generated may increase the system operating temperature more quickly. Active control of fuel cell stack operating pressure may also decrease the cold start transients. Electric or fuel-fired heaters could be evaluated to see if the heater energy used is offset by increased fuel cell efficiency.

Finally as seen in the performance limitations with the US06 drive cycle, fuel cell system size could be increased to decrease the cold start power limitations in the system. However, this modeling effort cannot predict the practical limitations (weight, size, cost) that may plague such a scenario.

REFERENCES

P. Atwood, S. Gurski, D. J. Nelson, and K. B. Wipke (2001), "Degree of Hybridization Modeling of a Fuel Cell Hybrid Electric Sport Utility Vehicle," SAE Paper 2001-01-0236, in *Fuel Cell Power for Transportation* 2001, SP-1589, pp. 23-30.

M. Fronk, Matthew H., David L. Wetter, David A. Masten, Transportation," SAE paper 2000-01-0373, in *Fuel Cell Power for Transportation* 2000, SAE SP 1505, pp.101 – 108.

Gurski, Stephen D. (2002), "Cold-Start Effects on Performance and Efficiency for Vehicle Fuel Cell Systems," MS Thesis, VPI&SU, Blacksburg, VA. Available on http://scholar.lib.vt.edu/theses/available/etd-12192002-162600/ .

D.G. Kroger, "Radiator Characterization and Optimization," SAE paper 840380, Vol. 93 *SAE Transactions*, 1984 pp. 2.984-2.990

G. Kulp and D.J. Nelson (2001), "A Comparison of Two Fuel Cell Air Compression Systems at Low Load", SAE paper 2001-01-2547 in Fuel Cells and Alternative Fuels/Energy Systems, SP-1635, *Proceedings of the 2001 SAE Future Transportation Technology Conference*, Costa Mesa, Ca., pp. 81-90

G. Kulp, S. Gurski, and D.J. Nelson (2002), "PEM Fuel Cell Air Management Efficiency at Part Load", *Proceedings of the 2002 Future Car Congress*, June 3-5, Arlington, VA, SAE paper 2002-01-1912, 14 pgs.

M. Sadler, R.P.G Heath and R.H. Thring "Warm Up Strategies for a Methanol Reformer Fuel Cell Vehicle," SAE paper 2000-01-0371, in *Fuel Cell Power for Transportation* 2000, SAE SP 1505, pp. 95 – 100.

ACKNOWLEDGEMENTS

We would like to thank CTTS analysis team especially Keith Wipke, Tony Markel, Kristina Harraaldson and Bill Kramer at the National Renewable Energy Laboratories for supporting this work under contract XCL-1-3116-01.

CONTACT INFORMATION

Dr. Douglas J. Nelson
Virginia Polytechnic Institute and State University
Mechanical Engineering Department
Blacksburg, Virginia 24061-0238
(540) 231-4324 Doug.Nelson@vt.edu